

Fusobacterium nucleatum GroEL induces risk factors of atherosclerosis in human microvascular endothelial cells and ApoE^{-/-} mice

H-R. Lee¹, H-K. Jun¹, H-D. Kim^{2,3}, S-H. Lee¹ and B-K. Choi^{1,3}

1 Department of Oral Microbiology and Immunology, School of Dentistry, Seoul National University, Seoul, Korea

2 Department of Preventive and Social Dentistry, School of Dentistry, Seoul National University, Seoul, Korea

3 Dental Research Institute, School of Dentistry, Seoul National University, Seoul, Korea

Correspondence: Bong-Kyu Choi, Department of Oral Microbiology and Immunology, School of Dentistry, Seoul National University, 28 Yongon-Dong, Chongno-Gu, Seoul 110-749, Korea Tel.: +82 2 740 8640; fax: +82 2 743 0311; E-mail: bongchoi@snu.ac.kr

Keywords: Atherosclerosis; GroEL; *Fusobacterium nucleatum*; periodontitis

Accepted 16 November 2011

DOI: 10.1111/j.2041-1014.2011.00636.x

SUMMARY

Infection and inflammation are risk factors in the initiation and progression of atherosclerosis. Periodontitis is one of the most prevalent chronic inflammations of the oral cavity, and has been reported to be associated with systemic disease. In this study, we evaluated whether the heat-shock protein GroEL of *Fusobacterium nucleatum*, one of the most prevalent bacteria in periodontitis, induces factors that predispose to atherosclerosis in human microvascular endothelial cells (HMEC-1) and apolipoprotein E-deficient (ApoE^{-/-}) mice. GroEL induced the expression of chemokines such as monocyte chemoattractant protein-1 and interleukin-8 as well as cell adhesion molecules, such as intercellular adhesion molecule 1, vascular cell adhesion molecule 1, and E-selectin. GroEL induced the activity of tissue factor and reduced the activity of the tissue factor pathway inhibitor. Foam cell formation was induced by GroEL. GroEL-injected ApoE^{-/-} mice showed significant atherosclerotic lesion progression compared with control mice. Serum levels of risk factors for atherosclerosis such as interleukin-6, C-reactive protein, and low-density lipoprotein were increased in GroEL-injected ApoE^{-/-} mice

compared with control mice, whereas serum levels of high-density lipoprotein were decreased. We could detect significantly higher levels of anti-*F. nucleatum* GroEL antibody in serum and *F. nucleatum* DNA in gingival crevicular fluid from patients with periodontitis than in that from healthy subjects. Our results indicate that the host response to the GroEL of periodontal pathogens like *F. nucleatum* may be a mechanism involved in atherosclerosis, supporting the association of periodontitis and systemic infection.

INTRODUCTION

Chronic infectious agents have been implicated in the pathogenesis of atherosclerosis. *Chlamydia pneumoniae*, *Helicobacter pylori*, herpes simplex virus and cytomegalovirus have been prominently associated with atherosclerosis (Leinonen & Saikku, 2002; Blum *et al.*, 2003; Campbell & Kuo, 2004; Ayada *et al.*, 2009). Recently, studies have shown not only that oral bacteria are found in other human body sites, but also that they are associated with systemic

diseases such as cardiovascular disease (CVD) and low-weight preterm birth (Seymour *et al.*, 2007). The association of chronic periodontitis with CVD has been postulated by the presence of periodontopathogens in atherosclerotic plaques. The high level of C-reactive protein (CRP) in the serum of patients with periodontitis and the decrease in systemic inflammation markers after treatment of periodontitis also underscore this association (Kozarov *et al.*, 2005; Tonetti *et al.*, 2007; Paraskevas *et al.*, 2008).

Fusobacterium nucleatum, a gram-negative anaerobe, is one of the most frequently found organisms in the subgingival plaque of patients with periodontitis. It has a pivotal role in dental biofilm formation by bridging early-colonizing commensals and late-colonizing pathogenic bacteria, so amplifying subgingival plaque maturation leading to periodontitis (Kolenbrander *et al.*, 2010). *Fusobacterium nucleatum* is invasive and belongs to the most frequently isolated species in amniotic fluid cultures from women with preterm labor and intact membranes (Hill, 1998; Han *et al.*, 2000, 2004). In an immunological study, *F. nucleatum* was found in human carotid endarterectomy specimens from patients undergoing surgical treatment of atherosclerosis (Ford *et al.*, 2006).

Bacterial GroEL is highly homologous with eukaryotic heat-shock protein 60 (HSP60) and is strongly immunogenic (Wick *et al.*, 2001). Because of its homologous nature with human HSP60 (hHSP60), GroEL can activate T cells with specificity for self-HSP60. Antibodies directed against bacterial GroEL cross-react with hHSP60 on endothelial cells, resulting in autoimmune responses that may lead to endothelial dysfunction and the development of atherosclerosis.

The objective of this study was to determine whether *F. nucleatum* GroEL induces factors predisposing to atherosclerosis in human microvascular endothelial cells (HMEC-1) and atherosclerotic lesions in ApoE^{-/-} mice.

METHODS

Bacterial culture

Fusobacterium nucleatum subsp. *nucleatum* (ATCC 25586) was grown in brain–heart infusion broth supplemented with 5 µg ml⁻¹ hemin (Sigma Chemical Co., St. Louis, MO) and 0.2 µg ml⁻¹ menadione

(Sigma Chemical Co.) under an anaerobic atmosphere (10% CO₂, 5% H₂, 85% N₂).

Cloning and expression of GroEL of *F. nucleatum*

The *groEL* gene was amplified from genomic DNA of *F. nucleatum* by polymerase chain reaction (PCR). The sequences of the primers used for PCR were 5'-AAC TGG ATC CAT GGC AAA AAT TAT AAA TTT TAA TG-3' and 5'-AAC TGA GCT CTT ACA TCA TTC CTG GCA TCA T-3'. The underlined sequences are the introduced restriction sites for *Bam*HI (GGATCC; Fermentas Inc., Glen Burnie, MD) and *Sac*I (GAGCTC; Fermentas Inc.), and four nucleotides were added to the 5' ends of these restriction sites. PCR amplification, cloning of the genes into *Escherichia coli* M15 using the expression vector pQE-30 predigested with *Bam*HI and *Sac*I, purification of the recombinant proteins with Ni-NTA agarose (Qiagen, Valencia, CA), and decontamination of endotoxin using polymyxin B agarose (Sigma Chemical Co.) were all performed as described previously (Lee *et al.*, 2005). The *F. nucleatum* GroEL was identified using a cross-reactive anti-hHSP60 antibody (Stressgen Biotechnologies Co., Ann Arbor, MI). To verify endotoxin decontamination in the recombinant GroEL, Toll-like receptor 4 (TLR4)-dependent nuclear factor-κB (NF-κB) activation, which is not inhibited by polymyxin B (Sigma Chemical Co.), was analysed using the CD25-expressing reporter cell line, Chinese hamster ovary (CHO) CD14-TLR4, and flow cytometry as described previously (Lee *et al.*, 2005). CHO-CD14-TLR4 cells have the gene encoding membrane CD25 with the human E-selectin promoter, which contains NF-κB binding sites (Han *et al.*, 2003). We also measured the endotoxin activity of GroEL by *Limulus* amoebocyte lysate assay using a LAL Endochrome Kit (Charles River Endosafe, Wilmington, MA) according to the manufacturer's protocol.

Sampling of sera and subgingival plaques

Patients with chronic periodontitis ($n = 10$) and periodontally healthy subjects ($n = 10$) were recruited for sampling serum and subgingival plaques. Periodontal status was evaluated by various clinical parameters, including periodontal probing depth, clinical attachment level, and residual tooth. The patients with chronic periodontitis had >3 mm probing depth and

>3 mm attachment loss, affecting at least one tooth in each quadrant. The study was performed according to the Declaration of Helsinki. The Institutional Review Board at Seoul National University approved the study, and written informed consent was obtained from all subjects. Venous blood samples were taken for analysis of serum levels of IgG antibody to *F. nucleatum* GroEL. Subgingival plaque samples were collected from the deepest site of the subjects by inserting three sterile paper points (size 20) in the gingival sulcus for 10 s as described previously (Choi *et al.*, 2000). The paper points were immediately placed in 1 ml phosphate-buffered saline (PBS) in 2-ml screw-cap microtubes and stored at -20°C until use.

Determination of anti-*F. nucleatum* GroEL antibody levels in human sera

To determine serum levels of anti-*F. nucleatum* GroEL antibody, serum samples were pre-absorbed with 1 ml cultured *Porphyromonas gingivalis* pellets at 4°C overnight and subsequently with $10\ \mu\text{g ml}^{-1}$ hHSP60 for 1 h at room temperature. Ninety-six-well microtiter plates (BD Falcon, Bedford, MA) were coated with *F. nucleatum* GroEL ($0.5\ \mu\text{g}$ in $50\ \mu\text{l}$ per well in $0.05\ \text{M}$ carbonate buffer, pH 9.6) overnight at 4°C . After washing three times with PBS containing 0.05% Tween-20 (PBS-T; AMRESCO Inc., Solon, OH), non-specific binding sites were blocked with PBS-T containing 3% casein for 2 h at room temperature. The plates were washed with PBS-T, and $50\ \mu\text{l}$ of 100-fold diluted pre-absorbed sera with PBS was added and incubated for 1 h at room temperature. After washing with PBS-T, the antibody levels were detected by adding horseradish peroxidase-conjugated goat anti-human IgG (R&D Systems, Minneapolis, MN) for 1 h and subsequently developing with 3,3',5,5'-tetramethylbenzidine (Sigma Chemical Co.) liquid substrate. The absorbance was measured at a wavelength of 450 nm using a VERSAmax Tunable Microplate Reader (Molecular Devices, Downingtown, PA). A standard curve using dilutions of human IgG (Sigma Chemical Co.) was used to calculate the levels of the antibodies.

Detection of *F. nucleatum* in subgingival plaques

The genomic DNA was extracted from the subgingival plaques using a genomic DNA extraction kit

(iNtRON Biotechnology, Seongnam, Korea) according to the manufacturer's instructions. *Fusobacterium nucleatum* DNA in the subgingival plaques was detected by quantitative PCR of 16S rDNA as described previously (Ryu *et al.*, 2010). The linearity and detection limits were determined by amplifying 10-fold serial dilutions of the genomic DNA of *F. nucleatum* as a standard and the standard curve and Ct values were used to calculate DNA amount in the samples. The sequences of the primers were 5'-CGC AGA AGG TGA AAG TCC TGT AT-3' for a forward primer and 5'-TGG TCC TCA CTG ATT CAC ACA GA-3' for a reverse primer. The specificity of the primers was tested against *Aggregatibacter actinomycetemcomitans*, *F. nucleatum* subsp. *nucleatum*, *P. gingivalis*, *Prevotella intermedia*, *Tannerella forsythia* and *Treponema denticola* by PCR. The 99-base-pair PCR product was observed only in *F. nucleatum*.

Treatment of HMEC-1 with GroEL and real-time reverse transcription-PCR

The HMEC-1 cells were cultured in MCDB131 medium (Gibco BRL, Paisley, UK) supplemented with 15% heat-inactivated fetal bovine serum (FBS; Thermochemical HyClone, Barrington, IL), antibiotics ($100\ \mu\text{g ml}^{-1}$ streptomycin and $100\ \text{U ml}^{-1}$ penicillin; Gibco BRL), $0.1\ \mu\text{g ml}^{-1}$ of hydrocortisone (Sigma Chemical Co.) and $0.1\ \mu\text{g ml}^{-1}$ epidermal growth factor (Invitrogen Life Technology, Carlsbad, CA). The cells were seeded onto six-well plates (BD Falcon) at a concentration of $2 \times 10^6\ \text{cells ml}^{-1}$ and cultured overnight. The cells were then stimulated with GroEL (5 and $10\ \mu\text{g ml}^{-1}$) for 12 h and 24 h. RNA isolation from the cells, cDNA synthesis and real-time reverse transcription (RT-PCR) was performed for detection of the mRNA expression of interleukin-8 (IL-8), monocyte chemoattractant protein 1 (MCP-1), intercellular adhesion molecule 1 (ICAM-1), vascular cell adhesion molecule 1 (VCAM-1), E-selectin and tissue factor (TF) as described previously (Jun *et al.*, 2008). Glyceraldehyde dehydrogenase (GADPH) was used as a reference to normalize expression levels. The primers for PCR were designed using PRIMER3 v. 0.4.0 program (<http://frodo.wi.mit.edu/primer3/>). The sequences of the primers for PCR were as follows: 5'-CAG CCA GAT GCA ATC AAT GC-3' and 5'-GTG GTC CAT GGA ATC CTG AA-3' for MCP-1; 5'-CAT

ATG CCA TGC AGC TAC AC-3' and 5'-AGT TGT ATG TCC TCA TGG TG-3' for ICAM-1; 5'-AAG CGG AGA CAG GAG ACA C-3' and 5'-TGG CAG GTA TTA TTA AGG AGG ATG-3' for VCAM-1; 5'-TGT GAG ATG CGA TGC TGT C-3' and 5'-AAC CTC TTC TGT CCA TTG TCC-3' for E-selectin; 5'-CAC CGA CGA GAT TGT GAA GGA T-3' and 5'-CCC TGC CGG GTA GGA GAA-3' for TF; and 5'-GTG GTG GAC CTG ACC TGC-3' and 5'-TGA GCT TGA CAA AGT GGT CG-3' for GADPH.

The cytotoxic effect of GroEL on HMEC-1 cells was analysed using Cell Counting Kit-8 (CCK-8) from Dojindo Molecular Technologies (Rockville, MD) according to the manufacturer's protocol.

Flow cytometric analysis for adhesion molecules on GroEL-treated HMEC-1

The HMEC-1 cells were seeded onto 12-well plates (BD Falcon) at a concentration of 2×10^5 cells per well and cultured overnight. The cells were stimulated with GroEL ($10 \mu\text{g ml}^{-1}$) for 12 h and 24 h and detached using Trypsin-EDTA (Gibco BRL). The cells were incubated with antibody against ICAM-1 (CD54, BD, Franklin Lakes, NJ), VCAM-1 (CD106; R&D Systems), or E-selectin (CD62E; R&D Systems) that conjugated with the green fluorescent fluorescein isothiocyanate (FITC). After 30 min incubation at 4°C , the cells were washed (4°C , 520 g, 5 min) and subjected to flow cytometry (BD FACScalibur, BD) to analyse surface-expressed ICAM-1, VCAM-1 and E-selectin.

ELISA for chemokine production in GroEL-treated HMEC-1

The level of IL-8 and MCP-1 in the culture supernatants of HMEC-1 cells treated with GroEL was measured using DuoSet[®] enzyme-linked immunosorbent assay (ELISA) Development Systems (R&D Systems) according to the manufacturer's instructions.

Effect of GroEL on monocyte adhesion to endothelial cells and transendothelial migration

For the adhesion assay THP-1 cells, a human monocyte cell line, were cultured in RPMI-1640 medium (Gibco-BRL) with 10% FBS and labeled with carboxy-fluorescein diacetate, succinimidyl ester (CFSE, Invi-

trogen Life Technology). CFSE-labeled THP-1 cells were stimulated with $10 \mu\text{g ml}^{-1}$ GroEL or *E. coli* lipopolysaccharide (LPS; Sigma Chemical Co.) for 12 h. In parallel, HMEC-1 cells were seeded in 96-well microtiter plates (BD Falcon) at 2.5×10^4 cells per well and cultured in MCDB131 medium supplemented with 15% FBS, 1% antibiotics ($100 \mu\text{g ml}^{-1}$ streptomycin and 100 U ml^{-1} penicillin), $0.1 \mu\text{g ml}^{-1}$ hydrocortisone and $0.1 \mu\text{g ml}^{-1}$ epidermal growth factor. The cells were cultured to confluence and stimulated with $10 \mu\text{g ml}^{-1}$ GroEL or *E. coli* LPS for 12 h. GroEL and LPS-treated THP-1 cells were washed with Dulbecco's PBS (DPBS, Gibco BRL), resuspended in RPMI-1640 medium (Gibco BRL) at a density of 1×10^6 cells per ml, and added to GroEL-treated or LPS-treated HMEC-1. Alternatively, non-stimulated THP-1 cells were added to GroEL-stimulated HMEC-1 cells and GroEL-stimulated THP-1 cells were added to non-stimulated HMEC-1 cells. After incubation for 12 h, non-adherent THP-1 cells were washed away with PBS. The adherent CFSE-labeled THP-1 cells were lysed and the fluorescence intensity was measured by using GloMax[®]-Multi Microplate Multimode Reader (Promega, Madison, WI). All experiments were performed in triplicate.

To evaluate monocyte transmigration across an endothelial monolayer, HMEC-1 cells were seeded into the upper chamber of Transwell culture plates (6.5 mm Transwell inserts with 8- μm pore size; Corning Life Sciences, Union City, CA) at a density of 5×10^4 cells per well and cultured to confluence. The confluence of endothelial monolayers was assessed by exclusion of trypan blue-bound bovine serum albumin (BSA) as described previously (Gudgeon & Martin, 1989). Briefly, $100 \mu\text{l}$ trypan blue-bound BSA (4%) was added onto transwell inserts containing endothelial monolayers and the amount of trypan blue-bound BSA in the lower chamber was measured using a spectrophotometer. HMEC-1 cells were stimulated with $10 \mu\text{g ml}^{-1}$ GroEL or *E. coli* LPS in medium for 24 h; in parallel, THP-1 cells (1×10^6 cells per ml) were stimulated with $10 \mu\text{g ml}^{-1}$ GroEL or LPS in serum-free medium for 24 h. After washing the upper chamber, GroEL- or LPS-stimulated THP-1 cells were added to the upper chamber at a density of 1×10^6 cells per well and incubated at 37°C for 20 h to allow transendothelial migration. This assay was also performed using GroEL-stimulated THP-1 cells/non-stimulated HMEC-1 or non-stimulated

THP-1 cells/GroEL-stimulated HMEC-1. The medium was taken from the lower chamber and migrated cells were counted under a microscope (CKX41; Olympus, Tokyo, Japan) using a cell-counting hemacytometer (Marinefeld, Lauda-Königshofen, Germany).

Tissue factor expression assay

To measure the surface expression level of TF in the endothelial cells, HMEC-1 cells (1×10^4 cells per well) were grown in 96-well plates to confluence. After washing with DPBS, the cells were treated with 1, 5 and $10 \mu\text{g ml}^{-1}$ *F. nucleatum* GroEL or $10 \mu\text{g ml}^{-1}$ *E. coli* LPS as a positive control for 12 h. After washing with DPBS, the cells were reacted with mouse anti-human TF monoclonal antibody (American Diagnostica Inc., Stamford, CT) for 1 h at room temperature. After washing with DPBS, the cells were fixed with 1% formaldehyde for 15 min. The cells were then washed with DPBS and incubated for 1 h with horseradish peroxidase-conjugated goat anti-mouse IgG (1 : 500 dilution) followed by developing with tetramethylbenzidine as described above. The absorbance was measured at a wavelength of 450 nm using a VERSAmax Tunable Microplate Reader.

Tissue factor procoagulant activity assay

To test whether the extent of TF induction correlated well with its activity, an Actichrome[®] TF Activity Assay Kit (American Diagnostica Inc.) was used. HMEC-1 cells were seeded onto a six-well plate at a concentration of 1×10^6 cells per well and incubated overnight. Cells were washed twice with DPBS and treated with 1, 5 and $10 \mu\text{g ml}^{-1}$ GroEL or $10 \mu\text{g ml}^{-1}$ *E. coli* LPS as a positive control for 24 h. The cells were harvested and sonicated in a buffer (pH 7.4) of 50 mM Tris-HCl, 100 mM NaCl and 0.1% Triton X-100. Tissue factor was extracted in the buffer for 30 min at 37°C. The TF activity was determined in cell extracts according to the manufacturer's instructions. Briefly, 50 μl assay buffer was added to each well in a 96-well round bottom plate (BD Falcon) and subsequently 25 μl lipidated TF standards and TF extracts of GroEL-treated HMEC-1 cell lysates were added to each well. Then 25 μl human factor VIIa and human factor X were added and incubated at 37°C for 15 min. For chromogenic observation, 25 μl Spectrozyme FXa, a fluorogenic substrate, was

added to each well and incubated at 37°C for 15 min. The color reaction was stopped by adding 50 μl glacial acetic acid, and the absorbance was read at a wavelength of 405 nm using VERSAmax Tunable Microplate Reader.

Tissue factor pathway inhibitor activity assay

To determine the effect of GroEL on TF pathway inhibitor (TFPI) activity, an Actichrome[®] TFPI Activity Assay Kit (American Diagnostica Inc.) was used. HMEC-1 cells were seeded onto the 48-well plate (BD Falcon) at a density of 1×10^5 cells per well and incubated overnight. Cells were washed twice with DPBS and treated with 1, 5 and $10 \mu\text{g ml}^{-1}$ GroEL or $10 \mu\text{g ml}^{-1}$ *E. coli* LPS for 24 h. TFPI activity in the cell culture supernatants was measured according to the manufacturer's instructions. Briefly, 20 μl TFPI standard, diluted reference plasma, or collected test supernatant, was added to each well of 96-well round-bottom plates. Then 20 μl TF/human factor VIIa complex was added to the wells and incubated at 37°C for 30 min. After incubation, 20 μl human factor X was added to each well and incubated at 37°C for an additional 15 min. Then 20 μl EDTA and Spectrozyme FXa substrate were sequentially added to each well. The detection of the color reaction was performed as described above.

Quantification of foam cell formation by GroEL

THP-1 cells were seeded on 24-well culture plates at a density of 1×10^5 cells per well and differentiated into macrophages using 100 nM phorbol 12-myristate 13-acetate (PMA; Sigma Chemical Co.) for 48 h. After washing with DPBS, the cells were cultured in fresh medium without PMA for 24 h, treated with 1, 5, $10 \mu\text{g ml}^{-1}$ GroEL or $10 \mu\text{g ml}^{-1}$ *E. coli* LPS for 2 h, and then incubated with $100 \mu\text{g ml}^{-1}$ human oxidized low-density lipoprotein (LDL; INTRACEL, Frederick, MD) for 20 h. We also included recombinant FadA, the surface protein of *F. nucleatum* (1, 5 and $10 \mu\text{g ml}^{-1}$, kindly provided by Y. Choi, Seoul National University, Korea) as a protein control. The cells were washed with serum-free medium, fixed with 4% paraformaldehyde for 20 min, and stained with 300 μl oil-red O (Sigma Chemical Co.) for 2 min. After washing with DPBS, the dye was solubilized with 200 μl isopropyl alcohol and the absorbance was

read at a wavelength of 510 nm using VERSAmax Tunable Microplate Reader. Foam cell formation was observed under a phase-contrast microscope (Eclipse TE200; Nikon, Tokyo, Japan).

Animal experiment

The animal experiment was approved by the Institutional Review Board at Seoul National University, and the study was conducted in accordance with the Guide for the Care and Use of Laboratory Animals published by the United States National Institutes of Health. Four-week-old ApoE^{-/-} spontaneously hyperlipidemic male mice were purchased from ORIENT Bio Inc. (Gyeonggi-do, Korea). They were fed a high-fat diet (TestDiet, Richmond, VA) and water. The ingredients (%) of the high-fat diet were as follows: mouse diet 75%, cocoa butter 7.5%, casein 7.5%, glucose 2.5%, sucrose 1.625%, dextrin 1.625%, powdered cellulose 1.25%, cholesterol 1.25%, AIN-76 mineral mix 0.875%, sodium cholate 0.5%, AIN-76A vitamin mix 0.25% and choline chloride 0.125%. After 6 weeks, the mice were randomly separated into three groups (four mice in each group). The first group was injected intraperitoneally (i.p.) every week for 8 weeks with 50 μ l PBS, the second group was injected i.p. every week for 8 weeks with 50 μ l live *F. nucleatum* (5×10^7 colony-forming units mouse⁻¹), and the last group was injected i.p. every week for 8 weeks with *F. nucleatum* GroEL (50 μ g in 50 μ l mouse⁻¹). All mice were monitored twice a week until sacrifice. The mice were anesthetized with avertin (2, 2, 2-tribromoethanol; Sigma Chemical Co.) in 2-methyl-2-butanol (Sigma Chemical Co.) at 19 weeks of age. Cardiac puncture was performed to collect whole body blood. The heart and aortic tree were perfused by injection with saline solution into the right or left atrium four or five times until the aorta was clear. Then the organ (from heart to aorta) was excised from the each mouse. Collected organs were washed with PBS and fixed in 4% paraformaldehyde overnight at 4°C. The organs were incubated in 20% sucrose solution for 3–6 h at 4°C to prevent tissue damage upon freezing, and were then embedded in tissue-freezing medium (Jung, Nussloch, Germany) for 10 min at 4°C. The frozen organs were cut carefully into 10- μ m-thick sections. The tissue sections were captured on glass slides that had been coated with 3-aminopropyltriethoxysilane (Sigma Chemical

Co.) in acetone and tissue-freezing medium. The slides were stored at -20°C until use. For immunohistological evaluation, the slides were prepared with oil-red O staining of lipid as described previously (Beattie *et al.*, 2009). The slides were observed using a microscope (BX51; Olympus) and the atherosclerotic lesions were measured using IMAGE J computer program by calculating lipid accumulation as a percentage of total plaque area formed in the proximal aorta.

Serum levels of anti-*F. nucleatum* GroEL antibody in mouse serum were detected using horseradish peroxidase-conjugated goat anti-mouse IgG (R&D Systems) as described above with human sera. A standard curve using dilutions of mouse IgG (Sigma Chemical Co.) was used to calculate the levels of the antibodies.

Determination of serum levels of IL-6, CRP and lipoproteins

Mouse serum samples were analysed for concentrations of IL-6, CRP, HDL and LDL using an IL-6 Immunoassay Kit (R&D Systems, Minneapolis, MN), a Mouse CRP ELISA Kit (Alpha Diagnostic Intl. Inc., San Antonio, TX) and HDL and LDL/VLDL Cholesterol Quantitation Kits (BioVision, Mountain View, CA) according to the manufacturer's protocols.

Statistical analysis

An unpaired Student's *t*-test was performed to compare untreated control and GroEL-treated experimental groups.

RESULTS

Preparation of recombinant GroEL

The *groEL* gene was cloned in *E. coli* using the expression vector pQE-30, and histidine-tagged recombinant GroEL was purified using a Ni-NTA agarose gel. Immunoblot analysis showed that anti-hHSP60 antibody cross-reacted with the recombinant GroEL and whole cell lysates of *F. nucleatum* with approximately 70-kDa molecular mass (data not shown). To verify that the recombinant GroEL was not contaminated with endotoxin, CHO cells transfected with TLR4 and CD14 that expressed mem-

brane-bound CD25 through TLR4-dependent NF- κ B activation were used to assess the response to recombinant GroEL and LPS in the presence of polymyxin B, an endotoxin inhibitor. Both GroEL and LPS are known to be ligands to TLR4, so GroEL and LPS were expected to increase the expression of CD25 in the CHO cells. Both GroEL and LPS increased CD25 expression (Fig. S1). However, LPS-induced CD25 expression was inhibited by polymyxin B, whereas GroEL-induced CD25 expression was not affected. The endotoxin activity of the recombinant GroEL was 0.38 endotoxin unit μg^{-1} of the protein and this activity was about 1/75,000 of the same amount of *E. coli* LPS, when measured by *Limulus* amoebocyte lysate assay. These results indicated that endotoxin contamination was minimal in the recombinant GroEL.

Increased serum antibody levels to *F. nucleatum* GroEL and *F. nucleatum* in subgingival plaques in periodontitis patients

Bacterial GroEL-like proteins are known to be immunogens and *F. nucleatum* is isolated more frequently from patients with periodontitis than from periodontally healthy subjects. So we analysed *F. nucleatum*

GroEL IgG levels in sera from 10 periodontally healthy subjects and 10 periodontitis patients after adsorption with *P. gingivalis* and hHSP60. As shown in Fig. 1A, the serum IgG levels were significantly higher in periodontitis patients than in healthy subjects.

To determine whether the increased antibody level against *F. nucleatum* GroEL was associated with increased bacterial number, we detected *F. nucleatum* in subgingival plaque taken from the same subjects used for serum collection by real-time RT-PCR. As shown in Fig. 1B, significantly more *F. nucleatum* DNA was detected in patients with periodontitis compared with healthy subjects.

Induction of chemokines, adhesion molecules and procoagulant factors by GroEL

To test whether *F. nucleatum* GroEL is involved in the pathogenesis of infection-induced atherosclerosis, we investigated the expression of chemokines, adhesion molecules and procoagulant factors. GroEL at the concentrations of 5 and 10 $\mu\text{g ml}^{-1}$ significantly upregulated mRNA expression of adhesion molecules such as ICAM-1, VCAM-1 and E-selectin, as well as

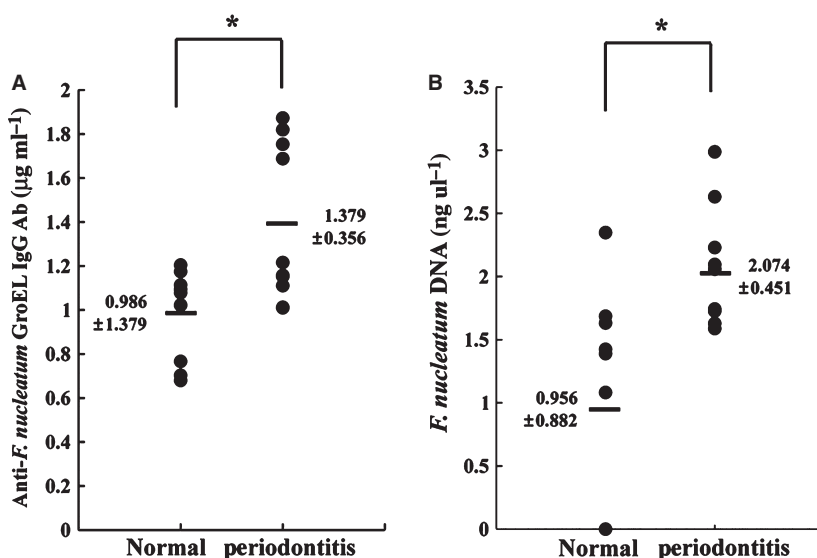


Figure 1 Levels of serum IgG to *Fusobacterium nucleatum* GroEL and *F. nucleatum* DNA. Levels of serum IgG to *F. nucleatum* GroEL in normal subjects ($n = 10$) and patients with periodontitis ($n = 10$) after adsorption against human heat-shock protein 60 (hSP60) and *Porphyromonas gingivalis* were determined by enzyme-linked immunosorbent assay using recombinant *F. nucleatum* GroEL as an antigen. *F. nucleatum* DNA level in subgingival plaques from normal subjects ($n = 10$) and patients with periodontitis ($n = 10$) was detected by real-time reverse transcription-polymerase chain reaction. *Statistical significance at $P < 0.05$ compared with healthy subjects. The mean \pm SD for each group is shown.

chemokines such as IL-8 and MCP-1 in HMEC-1 cells after 12 and 24-h treatment. Data from $10 \mu\text{g ml}^{-1}$ GroEL are shown in Fig. 2. The increase in chemokines and adhesion molecules induced by GroEL was confirmed at the protein level by detection via ELISA (IL-8 and MCP-1) and flow cytometry (ICAM-1, VCAM-1 and E-selectin). When analysed by flow cytometry, the expression level of VCAM-1 after 24-h treatment was lower than that after 12-h treatment and the expression level of ICAM-1 and E-selectin after 24-h treatment was slightly higher than that after 12-h treatment.

Tissue factor (also called Factor III) is involved in the extrinsic pathway of the coagulation system by interacting with factor VIIa, calcium ions and phospholipids to activate factor X to Xa, which then acts

on prothrombin according to the common pathway of coagulation (Morrissey, 2001). To determine the effect of GroEL on the expression of procoagulant activity, we analysed the expression and activity of TF and TFPI. Real-time RT-PCR analysis revealed that GroEL significantly stimulated the expression of TF mRNA in HMEC-1 cells in a dose-dependent manner compared with non-treated controls (Fig. 3A). The upregulated expression of TF was confirmed at the protein level by detection of GroEL-treated HMEC-1 cells with anti-TF IgG (Fig. 3B). To test whether the increased TF expression was correlated with its increased activity, we examined the procoagulant activity of GroEL-treated HMEC-1 cell lysates and observed approximately 2.1-fold and 3.7-fold increased TF activity in HMEC-1 cells treated with 5

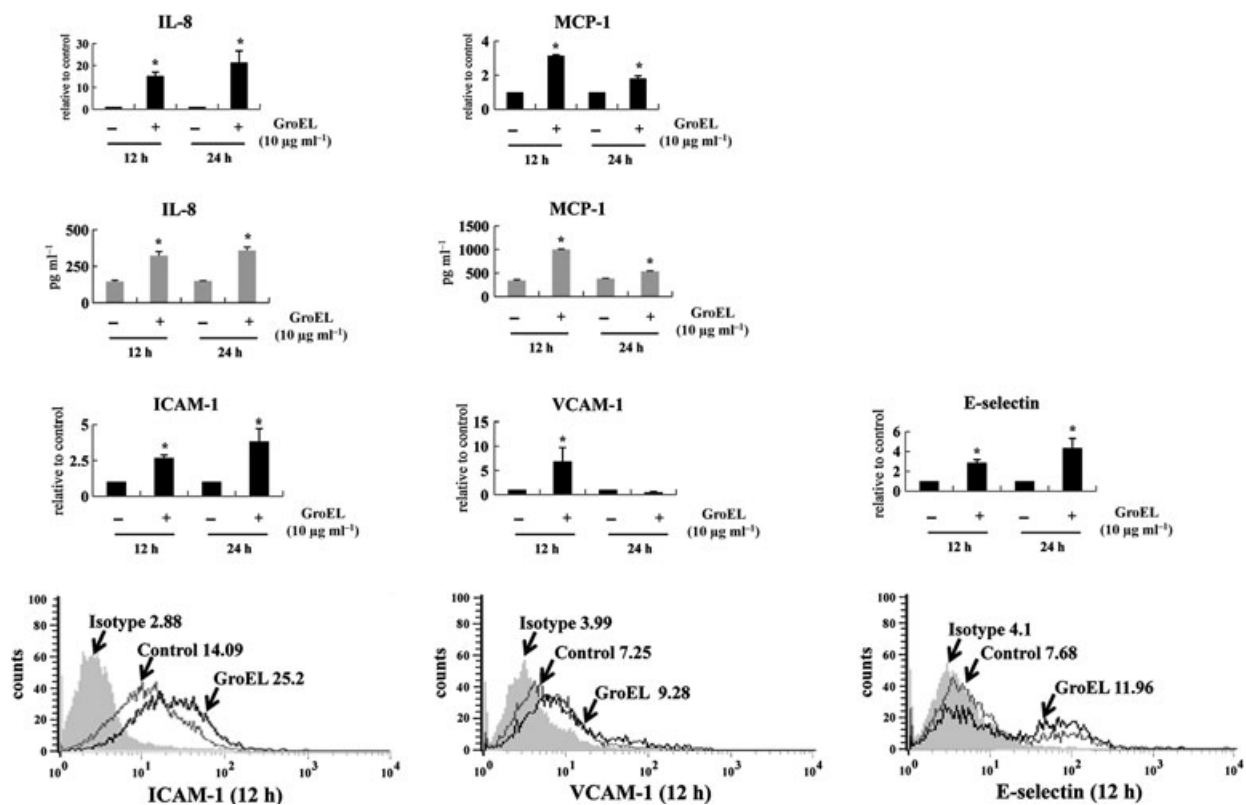


Figure 2 Induction of chemokines and adhesion molecules by *Fusobacterium nucleatum* GroEL in HMEC-1. HMEC-1 cells were treated with GroEL at a concentration of $10 \mu\text{g ml}^{-1}$ for 12 and 24 h. Total RNA was isolated from the cells and real-time reverse transcription–polymerase chain reaction was performed to detect expression of interleukin-8 (IL-8), monocyte chemoattractant protein 1 (MCP-1), intercellular adhesion molecule 1 (ICAM-1), vascular cell adhesion molecule 1 (VCAM-1) and E-selectin mRNA. The levels of IL-8 and MCP-1 in the culture supernatants, and ICAM-1, VCAM-1 and E-selectin expression on the cell surface were analysed by enzyme-linked immunosorbent assay and flow cytometry, respectively. The results of the flow cytometry analysis are presented as mean fluorescence intensity. The experiments were performed three times in triplicate and data from a representative experiment are shown. *Statistical significance at $P < 0.05$ compared with control.

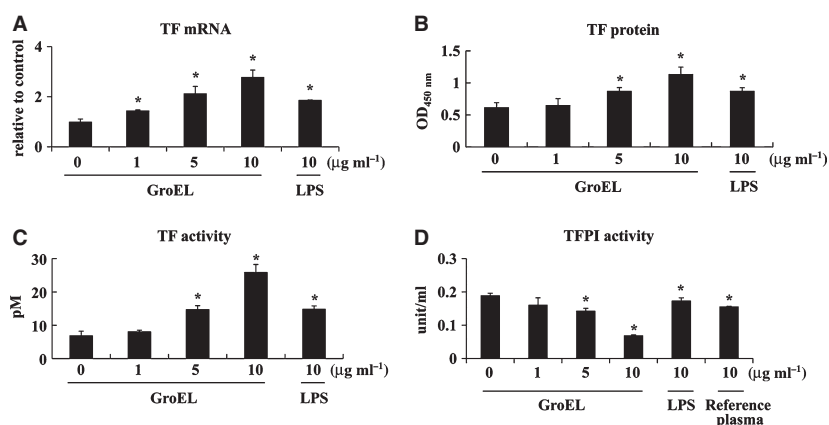


Figure 3 Effect of *Fusobacterium nucleatum* GroEL on tissue factor (TF) and TF pathway inhibitor (TFPI) in HMEC-1. (A) HMEC-1 cells were treated with GroEL for 12 h. Total RNA was isolated and real-time reverse transcription–polymerase chain reaction was performed to detect the expression of TF mRNA. (B) The expression of TF on the surface of HMEC-1 cells was measured using anti-human TF monoclonal antibody and horseradish peroxidase-conjugated secondary antibody. (C) For TF procoagulant activity, HMEC-1 cells were treated with GroEL for 24 h. Total cell lysates were assayed for procoagulant activity using a TF activity assay kit. (D) Cell culture supernatants of HMEC-1 cells treated with GroEL were harvested and a commercial TFPI activity assay kit was used to detect the anti-coagulant activity of secreted TFPI. Lipopolysaccharide (LPS) and reference plasma were used as positive controls. The experiments were performed three times in triplicate and data are shown as means \pm SD from a representative experiment. *Statistical significance at $P < 0.05$ compared with control.

and $10 \mu\text{g ml}^{-1}$ GroEL, respectively, compared with untreated cells (Fig. 3C). TFPI is the endogenous inhibitor of the TF-dependent pathway and an important regulator of coagulation. TFPI activity in HMEC-1 cells treated with GroEL was significantly reduced in a dose-dependent manner (Fig. 3D). These results indicate that GroEL increases procoagulant activity by upregulating TF and downregulating TFPI.

Recombinant GroEL showed no cytotoxic effect on HMEC-1 cells at the concentration used in this study (data not shown).

GroEL-enhanced adhesion to and migration of monocytes through an HMEC-1 monolayer

Monocyte adhesion to the luminal endothelium and the subsequent migration into the subendothelial layer of the intima is a critical step in atherosclerosis. As GroEL enhanced the cellular adhesion molecules (ICAM-1, VCAM-1 and E-selectin) and the chemokines (IL-8 and MCP-1) in HMEC-1, we tested whether GroEL increased monocyte adhesion to and the subsequent migration through the endothelial layer. For adhesion, CFSE-labeled THP-1 cells (a human monocyte cell line), which were either unstimulated or stimulated with GroEL, were added to an HMEC-1 monolayer that was also either unstimulated or stimu-

lated with GroEL. As shown in Fig. 4A, GroEL significantly increased THP-1 cell adhesion to the HMEC-1 cells. For transmigration, THP-1 cells were added to the upper chamber of the Transwell containing the HMEC-1 monolayers for 20 h. The transmigrated THP-1 cells were counted in the lower chamber. As shown in Fig. 4B, GroEL significantly increased the transmigration of THP-1 cells across an HMEC-1 monolayer. The confluence of the HMEC-1 monolayers was confirmed by restricted transfer of trypan blue-labeled albumin (Fig. S2). The highest efficacy of adhesion and translocation was observed when both cell types were stimulated with GroEL.

Increased foam cell formation induced by GroEL

Transmigrated monocytes found in the arterial intima differentiate into macrophages, most of which transform into foam cells (i.e. lipid-loaded macrophages). In the intima, macrophages take up lipoproteins, particularly oxidized LDL, forming foam cells that aggregate and form the atheromatous core. To evaluate the ability of GroEL to induce foam cell formation, PMA-differentiated THP-1 cells were pre-incubated with GroEL for 2 h before incubation with oxidized LDL. As shown in Fig. 5, GroEL significantly increased foam cell formation, which is evident by

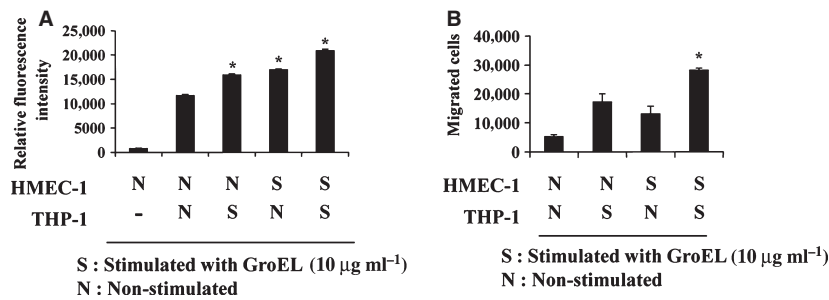


Figure 4 Increased activities of monocyte binding to HMEC-1 cells and transendothelial migration by GroEL. (A) HMEC-1 and CFSE-labeled THP-1 cells were treated with GroEL at a concentration of $10 \mu\text{g ml}^{-1}$ for 12 h. THP-1 cells were placed on the HMEC-1 cells that were grown in 96-well plates and allowed to bind for 12 h. The adherent cells were lysed and the fluorescence intensity was measured using a fluorometer. (B) Transendothelial migration was analysed using a Transwell system. THP-1 cells were added to the upper insert that contained an HMEC-1 monolayer and allowed to migrate for 20 h. The migrated cells were counted using a hemocytometer. The experiments were performed three times in triplicate and data are shown as means \pm SD from a representative experiment. *Statistical significance at $P < 0.05$ compared with control. NS, non-stimulated; S, stimulated with GroEL.

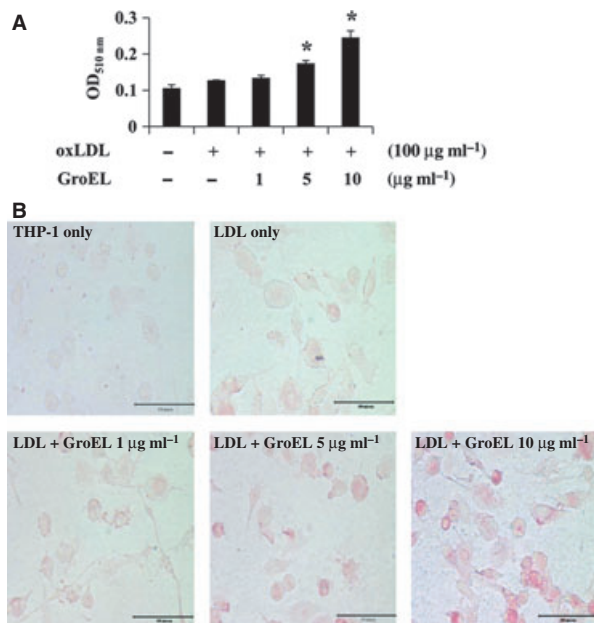


Figure 5 Foam cell formation induced by GroEL in differentiated THP-1 cells. PMA-differentiated THP-1 cells were incubated with *Fusobacterium nucleatum* GroEL. After low-density lipoprotein (LDL; $100 \mu\text{g ml}^{-1}$) was added and incubated for 20 h, the cells were washed with phosphate-buffered saline (PBS), fixed, and stained with oil-red O. (A) Lipid droplets that had accumulated in the cytoplasm were released using isopropyl alcohol and measured at 510 nm. The experiments were performed three times in triplicate and data are shown as means \pm SD from a representative experiment. *Statistical significance at $P < 0.05$ compared with cells treated with only LDL. (B) Foam cell formation was observed by phase contrast-microscopy (40 \times magnification).

the engulfment of oil red O lipid droplets in the macrophages, compared with cells incubated with LDL in the absence of GroEL. We also included recombi-

nant *F. nucleatum* FadA to test its ability to induce foam cell formation as a protein control to GroEL. FadA is an adhesin of *F. nucleatum* and involved in attachment to epithelial cells (Han *et al.*, 2005). FadA did not induce foam cell formation (data not shown).

Increased aortic lipid deposition in ApoE^{-/-} mice by *F. nucleatum* and GroEL

We evaluated atherosclerotic plaque accumulation by *F. nucleatum* and GroEL in ApoE^{-/-} spontaneously hyperlipidemic mice. Mice were treated i.p. with *F. nucleatum*, GroEL, or PBS once a week for 8 weeks then sacrificed at 19 weeks of age. Arterial lipid accumulation was detected by oil red O staining of a cryosection of the aortic root. All mice, including the PBS-treated control mice, showed accumulation of fibrous plaques on the intimal surface of the root. However, mice challenged with *F. nucleatum* or GroEL showed significantly increased lipid deposits in plaques compared with control animals (Fig. 6A,B). One animal in the control group died during the experiments and was omitted from the analysis.

To see the development of antibodies against *F. nucleatum* GroEL, the antibody levels were quantified in the serum samples of ApoE^{-/-} mice injected with GroEL or *F. nucleatum*. As shown in Fig. 6C, anti-GroEL antibody levels tended to slightly increase in the *F. nucleatum*-treated group and markedly increase in the GroEL-treated group compared with the PBS-treated control group. As a result of the limited serum

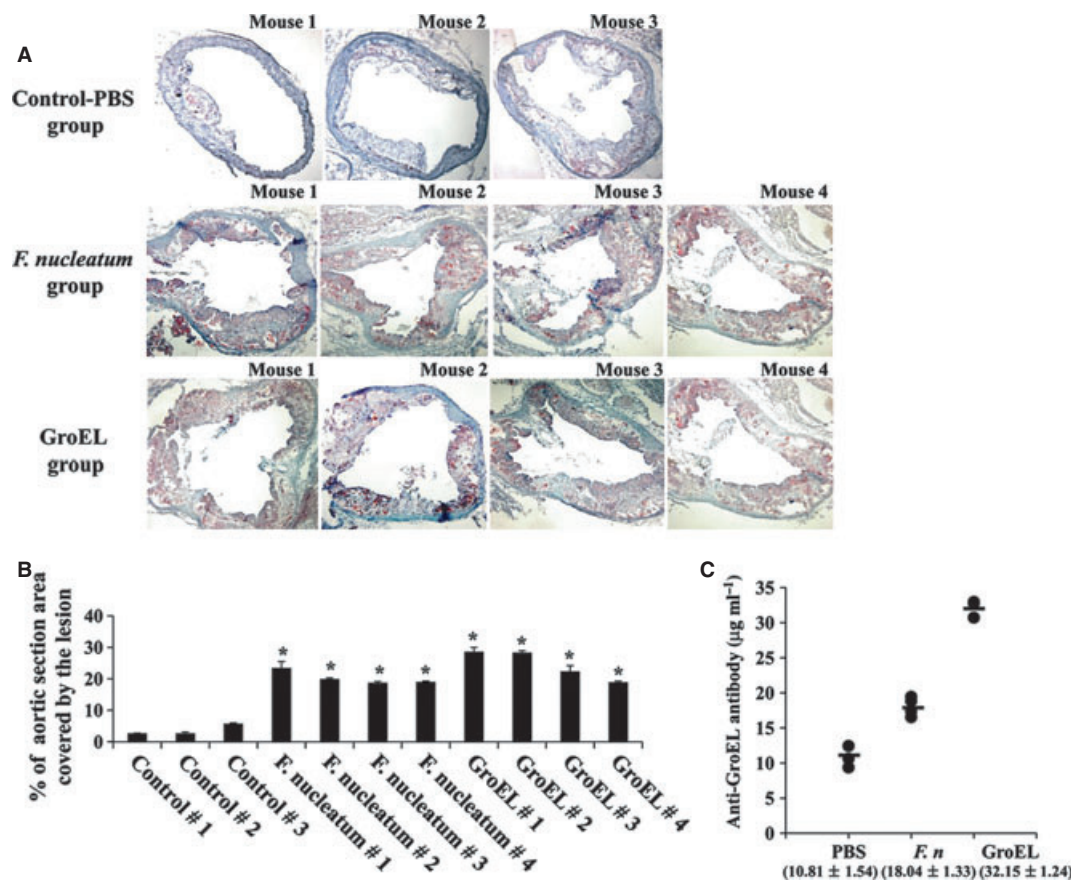


Figure 6 Atherosclerotic lesions in the proximal aorta of apolipoprotein E-deficient (ApoE^{-/-}) mice and development of anti-GroEL antibody. (A) The 10-week-old male mice were fed a high-fat diet and injected intraperitoneally with 50 µl phosphate-buffered saline (PBS; *n* = 3), 50 µl live *Fusobacterium nucleatum* (5×10^7 colony-forming units mouse⁻¹, *n* = 4) and GroEL (50 µg, *n* = 4) once a week for 8 weeks. Mice were killed at 19 weeks of age, and cryosections (10 µm) of the proximal aortas were stained with oil-red O and counterstained with hematoxylin to reveal lipid deposition; 40× magnification. (B) Oil-red O-stained lipid deposition was quantified with a computer-assisted image analysis system, IMAGE J. The extent of atherosclerosis was expressed as the percentage of total plaque area formed in the proximal aorta comprised by the lipid accumulated area. The mean ± SD for each group is shown in parenthesis. *Statistical significance at *P* < 0.05 compared with control. (C) Anti-GroEL antibody levels were detected in the serum samples of ApoE^{-/-} mice injected with GroEL or *F. nucleatum* by enzyme-linked immunosorbent assay. The mean ± SD for each group is shown.

amounts available, one sample from the GroEL-treated group was omitted from the analysis.

Serum analysis of mice injected with *F. nucleatum* and GroEL

Interleukin-6 and CRP are inflammatory indicators, and increased LDL levels and decreased HDL levels reflect an increased risk of atherosclerosis. As shown in Fig. 7, significantly higher serum levels of IL-6, CRP and LDL were detected in *F. nucleatum*-treated or GroEL-treated mice than in PBS-treated control mice. The HDL serum level was significantly lower in both *F. nucleatum*-treated and GroEL-treated mice than in control mice.

DISCUSSION

This study demonstrated that *F. nucleatum* GroEL stimulated atherosclerotic risk factors in HMEC-1 cells and in an ApoE^{-/-} mouse model, supporting the association of periodontal pathogens with atherosclerosis.

The etiology of CVD, including atherosclerosis, is complex. Both genetic and environmental factors play a role. In addition to these conventional risk factors, studies over the past few decades have suggested that infection and inflammation play an important role in the initiation and progression of atherosclerosis (Libby, 2002; Seymour *et al.*, 2007). Periodontal

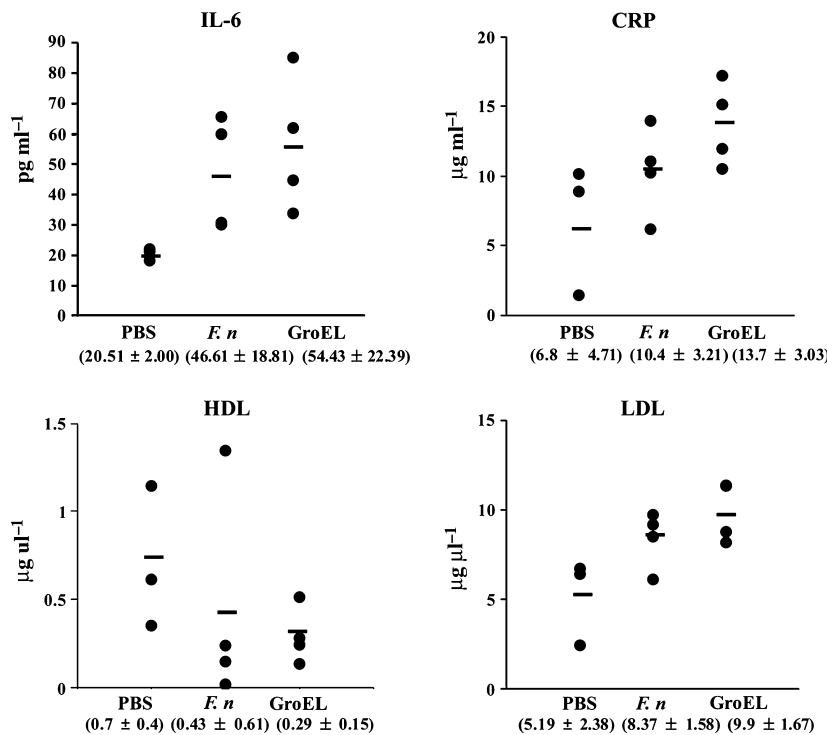


Figure 7 Serum levels of interleukin-6 (IL-6), C-reactive protein (CRP), low-density lipoprotein (LDL), and high-density lipoprotein (HDL) in apolipoprotein-deficient (ApoE^{-/-}) mice injected with *Fusobacterium nucleatum* and GroEL. The *F. nucleatum* or GroEL-injected mouse serum samples were collected as described in Methods and the levels of IL-6, CRP, LDL and HDL were detected by enzyme-linked immunosorbent assay. The mean ± SD for each group is shown.

pathogens can enter the circulation through tooth brushing, periodontal therapy, tooth extraction and endodontic treatment. These entry paths cause polymicrobial bacteremia that may produce endothelial inflammation, leading to atheroma development (Lockhart *et al.*, 2008).

Three major mechanisms have been postulated to link periodontitis with CVD: (i) direct invasion of the vascular endothelium by periodontopathogens; (ii) inflammation caused by immunological response to the pathogens and their products in the vascular endothelium; (iii) autoimmune response via molecular mimicry between bacterial antigens and self-antigens (Wick *et al.*, 2001; Seymour *et al.*, 2007). As a consequence of the homologous nature of hHSP60 and bacterial GroEL, hHSP60 on endothelial cells could activate hHSP60-specific T cells and cross-react with antibodies to bacterial GroEL. This cross-reactivity in the immune response may result in endothelial dysfunction followed by the development of atherosclerosis. GroEL is regarded as the primary antigen that may cause an autoimmune response via molecular

mimicry. GroEL is also an immunodominant antigen in patients with periodontitis. A positive relationship between periodontitis and the level of serum antibody directed to GroEL has been observed (Tabeta *et al.*, 2000). Immunohistological findings have confirmed the presence of bacterial GroEL and major periodontopathogens, including *F. nucleatum*, *P. gingivalis*, *T. forsythia*, *P. intermedia* and *A. actinomycetemcomitans*, in atherosclerotic lesions (Ford *et al.*, 2006). Similar to our results with *F. nucleatum* GroEL, the reactivity of *P. gingivalis* GroEL was higher in sera from patients with periodontitis than in sera from healthy subjects (Tabeta *et al.*, 2000). The level of anti-*P. gingivalis* GroEL antibodies was higher in atherosclerosis patients with advanced periodontal disease than in periodontally healthy patients with atherosclerosis (Ford *et al.*, 2005). *Porphyromonas gingivalis* GroEL-reactive T cells are present in the peripheral blood of patients with atherosclerosis and in atherosclerotic lesions, increasing the risk of atherosclerosis (Yamazaki *et al.*, 2004). Taken together, these findings suggest that increased

GroEL in periodontitis may play an important role in the initiation of atherosclerosis. The amino acid sequence of *F. nucleatum* GroEL has 50% identity/70% similarity with hHSP60 and 61% identity/79% similarity with *P. gingivalis* GroEL. The levels of anti-*F. nucleatum* GroEL antibody in human serum after absorption against HSP60 and *P. gingivalis* were decreased to 69% in healthy subjects and 40% in periodontitis patients compared with those before absorption. Even after this absorption, the detected levels of antibody against *F. nucleatum* GroEL may not exclude the presence of GroEL of other periodontopathogens because of their systemic presence. The high degree of homology between GroELs of periodontopathogens makes it likely that their immune and inflammatory responses could be conserved.

An association between periodontal pathogens such as *A. actinomycetemcomitans* and *P. gingivalis* and increased risk of CVD has been reported (Gibson *et al.*, 2004; Kozarov *et al.*, 2005; Zhang *et al.*, 2010), and epidemiological studies of the presence of GroEL were conducted in patients with atherosclerosis. However, the functional role of GroEL in atherosclerosis was not studied as thoroughly as in our study. In *P. gingivalis*, FimA plays an important role in invasion and accelerates atherosclerosis. Oral challenge of wild-type *P. gingivalis* resulted in increased atherosclerotic plaques in ApoE^{-/-} mice. The invasion-deficient FimA-mutant did not show similar results, although both strains were found in blood and aortic arch tissue of the animal (Gibson *et al.*, 2004). *Porphyromonas gingivalis* invasion is critical in the progression of atherosclerosis and *F. nucleatum* can bind to and invade epithelial and endothelial cells (Han *et al.*, 2000, 2004; Xu *et al.*, 2007).

GroEL of *F. nucleatum* increased the TF level and activity in our study. TF, also called Factor III, is a 47-kDa receptor glycoprotein and a highly inflammatory protein. Higher TF expression was observed in symptomatic atherosclerotic carotid arteries taken from patients who had recently had an ischemic stroke and in *C. pneumoniae*-infected carotid arteries (Stintzing *et al.*, 2005). An increase in TF was also observed in hHSP70, *C. pneumoniae* 60-kDa HSP, herpes simplex virus and cytomegalovirus (Visseren *et al.*, 2000; Benagiano *et al.*, 2005). *Porphyromonas gingivalis* increased TF activity and decreased TFPI levels in human aortic endothelial cells, but the

molecules to increase these factors have not been elucidated (Roth *et al.*, 2006).

The ApoE^{-/-} hyperlipidemic mouse is used to observe the entire spectrum of lesions seen during atherogenesis in humans (Nakashima *et al.*, 1994). In ApoE^{-/-} mice, we observed increased atherosclerotic lesions after GroEL and *F. nucleatum* injection. In addition, increased levels of IL-6, CRP and LDL and decreased HDL levels in mice treated with GroEL reflect inflammation and predisposing condition to atherosclerosis. These results support our *in vitro* data using HMEC-1 cells.

In summary, *F. nucleatum* GroEL upregulated the expression of chemokines, cell adhesion molecules and procoagulant factors. It also induced monocyte adhesion to and transmigration through endothelial cells in concert with increased uptake of lipids in atherosclerotic lesions. Our results indicate that the host response to GroEL of periodontal pathogens may be a mechanism involved in atherosclerosis and strongly support the association of periodontitis and systemic infections.

ACKNOWLEDGEMENTS

This work was supported by the National Research Foundation of Korea (NRF) grant funded by the Korean government (MEST) (2009-0075889).

REFERENCES

- Ayada, K., Yokota, K., Kobayashi, K., Shoenfeld, Y., Matsuura, E. and Oguma, K. (2009) Chronic infections and atherosclerosis. *Clin Rev Allergy Immunol* **37**: 44–48.
- Beattie, J.H., Duthie, S.J., Kwun, I.S., Ha, T.Y. and Gordon, M.J. (2009) Rapid quantification of aortic lesions in apoE^{-/-} mice. *J Vasc Res* **46**: 347–352.
- Benagiano, M., D'Elia, M.M., Amedei, A. *et al.* (2005) Human 60-kDa heat shock protein is a target autoantigen of T cells derived from atherosclerotic plaques. *J Immunol* **174**: 6509–6517.
- Blum, A., Peleg, A. and Weinberg, M. (2003) Anti-cytomegalovirus (CMV) IgG antibody titer in patients with risk factors to atherosclerosis. *Clin Exp Med* **3**: 157–160.
- Campbell, L.A. and Kuo, C.C. (2004) *Chlamydia pneumoniae*—an infectious risk factor for atherosclerosis? *Nat Rev Microbiol* **2**: 23–32.

- Choi, B.K., Park, S.H., Yoo, Y.J. et al. (2000) Detection of major putative periodontopathogens in Korean advanced adult periodontitis patients using a nucleic acid-based approach. *J Periodontol* **9**: 1387–1394.
- Ford, P.J., Gemmell, E., Hamlet, S.M. et al. (2005) Cross-reactivity of GroEL antibodies with human heat shock protein 60 and quantification of pathogens in atherosclerosis. *Oral Microbiol Immunol* **20**: 296–302.
- Ford, P.J., Gemmell, E., Chan, A. et al. (2006) Inflammation, heat shock proteins and periodontal pathogens in atherosclerosis: an immunohistologic study. *Oral Microbiol Immunol* **21**: 206–211.
- Gibson, F.C. III, Hong, C., Chou, H.H. et al. (2004) Innate immune recognition of invasive bacteria accelerates atherosclerosis in apolipoprotein E-deficient mice. *Circulation* **109**: 2801–2806.
- Gudgeon, J.R. and Martin, W. (1989) Modulation of arterial endothelial permeability: studies on an *in vitro* model. *Br J Pharmacol* **98**: 1267–1274.
- Han, Y.W., Shi, W., Huang, G.T. et al. (2000) Interactions between periodontal bacteria and human oral epithelial cells: *Fusobacterium nucleatum* adheres to and invades epithelial cells. *Infect Immun* **68**: 3140–3146.
- Han, S.H., Kim, J.H., Martin, M., Michalek, S.M. and Nahm, M.H. (2003) Pneumococcal lipoteichoic acid (LTA) is not as potent as staphylococcal LTA in stimulating Toll-like receptor 2. *Infect Immun* **71**: 5541–5548.
- Han, Y.W., Redline, R.W., Li, M., Yin, L., Hill, G.B. and McCormick, T.S. (2004) *Fusobacterium nucleatum* induces premature and term stillbirths in pregnant mice: implication of oral bacteria in preterm birth. *Infect Immun* **72**: 2272–2279.
- Han, Y.W., Ikegami, A., Rajanna, C., Kawsar, H.I., Zhou, Y. and Li, M. (2005) Identification and characterization of a novel adhesin unique to oral fusobacteria. *J Bacteriol* **187**: 5330–5340.
- Hill, G.B. (1998) Preterm birth: associations with genital and possibly oral microflora. *Ann Periodontol* **3**: 222–232.
- Jun, H.K., Kang, Y.M., Lee, H.R., Lee, S.H. and Choi, B.K. (2008) Highly conserved surface proteins of oral spirochetes as adhesins and potent inducers of proinflammatory and osteoclastogenic factors. *Infect Immun* **76**: 2428–2438.
- Kolenbrander, P.E., Palmer, R.J. Jr, Periasamy, S. and Jakubovics, N.S. (2010) Oral multispecies biofilm development and the key role of cell–cell distance. *Nat Rev Microbiol* **8**: 471–480.
- Kozarov, E.V., Dorn, B.R., Shelburne, C.E., Dunn, W.A. Jr and Progulske-Fox, A. (2005) Human atherosclerotic plaque contains viable invasive *Actinobacillus actinomycetemcomitans* and *Porphyromonas gingivalis*. *Arterioscler Thromb Vasc Biol* **25**: e17–e18.
- Lee, S.H., Kim, K.K. and Choi, B.K. (2005) Upregulation of intercellular adhesion molecule 1 and proinflammatory cytokines by the major surface proteins of *Treponema maltophilum* and *Treponema lecithinolyticum*, the phylogenetic group IV oral spirochetes associated with periodontitis and endodontic infections. *Infect Immun* **73**: 268–276.
- Leinonen, M. and Saikku, P. (2002) Evidence for infectious agents in cardiovascular disease and atherosclerosis. *Lancet Infect Dis* **2**: 11–17.
- Libby, P. (2002) Inflammation in atherosclerosis. *Nature* **420**: 868–874.
- Lockhart, P.B., Brennan, M.T., Sasser, H.C., Fox, P.C., Paster, B.J. and Bahrani-Mougeot, F.K. (2008) Bacteremia associated with toothbrushing and dental extraction. *Circulation* **117**: 3118–3125.
- Morrissey, J.H. (2001) Tissue factor: an enzyme cofactor and a true receptor. *Thromb Haemost* **86**: 66–74.
- Nakashima, Y., Plump, A.S., Raines, E.W., Breslow, J.L. and Ross, R. (1994) ApoE-deficient mice develop lesions of all phases of atherosclerosis throughout the arterial tree. *Arterioscler Thromb* **14**: 133–140.
- Paraskevas, S., Huizinga, J.D. and Loos, B.G. (2008) A systematic review and meta-analyses on C-reactive protein in relation to periodontitis. *J Clin Periodontol* **35**: 277–290.
- Roth, G.A., Moser, B., Huang, S.J., Brandt, J.S., Huang, Y. and Papananou, P.N. (2006) Infection with a periodontal pathogen induces procoagulant effects in human aortic endothelial cells. *J Thromb Haemost* **4**: 2256–2261.
- Ryu, J.I., Oh, K. and Yang, H. et al. (2010) Health behaviors, periodontal conditions, and periodontal pathogens in spontaneous preterm birth: a case-control study in Korea. *J Periodontol* **81**: 855–863.
- Seymour, G.J., Ford, P.J., Cullinan, M.P., Leishman, S. and Yamazaki, K. (2007) Relationship between periodontal infections and systemic disease. *Clin Microbiol Infect* **13**: 3–10.
- Stintzing, S., Heuschmann, P., Barbera, L. et al. (2005) Overexpression of MMP9 and tissue factor in unstable carotid plaques associated with *Chlamydia pneumoniae*, inflammation, and apoptosis. *Ann Vasc Surg* **19**: 310–319.
- Tabeta, K., Yamazaki, K., Hotokezaka, H., Yoshie, H. and Hara, K. (2000) Elevated humoral immune response to

- heat shock protein 60 (hsp60) family in periodontitis patients. *Clin Exp Immunol* **120**: 285–293.
- Tonetti, M.S., D’Aiuto, F., Nibali, L., Donald, A., Storry, C. and Parkar, M. (2007) Treatment of periodontitis and endothelial function. *N Engl J Med* **356**: 911–920.
- Visseren, F.L., Bouwman, J.J., Bouter, K.P., Diepersloot, R.J., de Groot, P.H. and Erkelens, D.W. (2000) Procoagulant activity of endothelial cells after infection with respiratory viruses. *Thromb Haemost* **84**: 319–324.
- Wick, G., Perschinka, H. and Millonig, G. (2001) Atherosclerosis as an autoimmune disease: an update. *Trends Immunol* **22**: 665–669.
- Xu, M., Yamada, M., Li, M., Liu, H., Chen, S.G. and Han, Y.W. (2007) FadA from *Fusobacterium nucleatum* utilizes both secreted and nonsecreted forms for functional oligomerization for attachment and invasion of host cells. *J Biol Chem* **282**: 25000–25009.
- Yamazaki, K., Ohsawa, Y., Itoh, H. *et al.* (2004) T-cell clonality to *Porphyromonas gingivalis* and human heat shock protein 60s in patients with atherosclerosis and periodontitis. *Oral Microbiol Immunol* **19**: 160–167.
- Zhang, T., Kurita-Ochiai, T., Hashizume, T., Du, Y., Ogu-chi, S. and Yamamoto, M. (2010) *Aggregatibacter actinomycetemcomitans* accelerates atherosclerosis with an increase in atherogenic factors in spontaneously hyperlipidemic mice. *FEMS Immunol Med Microbiol* **59**: 143–151.

SUPPORTING INFORMATION

Additional supporting information may be found in the online version of this article:

Figure S1. Flow cytometric analysis of Toll-like receptor 4 (TLR4)-dependent CD25 expression via stimulation of nuclear factor- κ B (NF- κ B) reporter in Chinese hamster ovary (CHO) cells by GroEL. CHO cells (CHO/CD14/TLR4) containing the gene encoding membrane CD25 with the human E-selectin promoter, which contains NF- κ B binding sites, were treated with GroEL ($10 \mu\text{g ml}^{-1}$) or *Escherichia coli* lipopolysaccharide (LPS; $10 \mu\text{g ml}^{-1}$) for 16 h in the presence or absence of polymyxin B ($50 \mu\text{g ml}^{-1}$). CD25 expression was analysed by flow cytometry using FITC-conjugated anti-human CD25 monoclonal antibody. The results are presented as mean fluorescence intensity.

Figure S2. Transfer of trypan blue-labeled albumin across confluent monolayers of HMEC-1 cells grown on Transwell inserts. Different number of HMEC-1 cells were seeded onto Transwell inserts and grown to confluence. Trypan blue-labeled bovine serum albumin (BSA; $100 \mu\text{l}$, 4%) was added to HMEC-1 monolayers formed on transwell inserts for 2 h and the amount of trypan blue-labeled BSA in the lower chamber was measured using a spectrophotometer. For transmigration experiments, cells were used at a density of 5×10^4 cells per well.

Please note: Wiley-Blackwell are not responsible for the content or functionality of any supporting materials supplied by the authors. Any queries (other than missing material) should be directed to the corresponding author for the article.

Copyright of Molecular Oral Microbiology is the property of Wiley-Blackwell and its content may not be copied or emailed to multiple sites or posted to a listserv without the copyright holder's express written permission. However, users may print, download, or email articles for individual use.